Study of a CI Engine for Off-Road Application in Diesel-Hydrogen Dual Fuel Configuration

Raphaël Gelé, Ezio Mancaruso, Salvatore Rossetti, Christine Rousselle, Pierre Brequigny

2025-24-0055

Study of a CI engine for off-road application in diesel-hydrogen dual fuel configuration

Raphaël Gelé[1], Ezio Mancaruso[2], Salvatore Rosetti[2], Christine Mounaïm-Rousselle[1], Pierre Brequigny[1]

[1] Université d'Orléans, INSA CVL, PRISME, UR 4229, F-45072, Orléans, France

[2] Consiglio Nazionale delle Ricerche Istituto di Scienze e Tecnologie per l'Energia e la Mobilit` a Sostenibili, CNR-STEMS, Via Marconi 4, 80125 Napoli, Italy

Abstract

Hydrogen as fuel in internal combustion engines is a promising solution for reducing greenhouse gas emissions, as its combustion produces only water vapor. One potential application is in dual fuel (DF) engines, where diesel is used to ignite the mixture, and hydrogen serves as the primary fuel. However, there is limited literature on the use of hydrogen in compression ignition (CI) engines for off-road applications running in dual fuel diesel/hydrogen, which motivates this study. The focus is on a 3-cylinder, 1-liter naturally aspirated (NA) engine with a compression ratio of 17.5:1 equipped with direct injection (DI) for diesel. Retrofitting the engine with 3 port fuel injectors, it was possible to feed the engine with hydrogen by the control system elaborated in the laboratory. The study aims to analyze dual fuel diesel/hydrogen combustion characteristics and the emissions across different engine speeds (from 1600 rpm to 3600 rpm) and loads (30%, 50% and 70%). The dual fuel operation was done by using 10% of the maximum load provided by diesel, and the overall load is adjusted by increasing the hydrogen amount. Engine load was managed up to a premixed ratio between 39% to 65% of energy provided by hydrogen, depending on the engine speed. The results indicate that the premixed charge of hydrogen burns differently, driven by diesel fuel. This behavior depends on the effective excess of air in the engine. Comparing the emissions in dual fuel configuration where 10% of the load is provided by diesel and diesel operation at the same engine power, CO_2 and NO_x emissions decrease up to 57% and 61%, respectively, for 70% load. On the other hand, particulate matter (PM) increases up to 77%, at 50% load; it can depend on the worsening of mixing and combustion of the main injection and less production but also less oxidation of the soot.

Introduction

Global warming, which is one of the effects of climate change, is manifested by the global increase of the temperature on earth due to human activities. The main cause of this climate change is the greenhouse effect. Some gases in the atmosphere trap the heat from the sun, causing the overall temperature to increase [1]. These gases are naturally produced by organisms on earth, but human activity has accelerated this production which increases the greenhouse effect. CO_2 is the main contributor to the greenhouse effect, accounting for 80.6% greenhouse gas emissions in 2022. It is also noted that the transport sector is the 2nd largest emitter of CO_2 with 23.8% of global emissions in 2022 in the world [2]. Because every ton of CO_2 emitted contributes to global warming, it is important to reduce these emissions to slow down the rise in temperatures. The CO_2 emitted is mainly from the use of carbon-based fuel in combustion engines. The use of bio-sourced fuels and carbon-free fuels is one efficient solution to participate in the decarbonization of the transport sector.

Hydrogen is one promising fuel for internal combustion engines. It is a zero-carbon fuel that can be produced from several sources [3]. such as electrolysis, gasification of biomass, or transformation of other gas using thermochemical process. All these production methods can use renewable energies, meaning that hydrogen can have almost zero carbon impact from its production to its use. Hydrogen has some interesting characteristics for its use in internal combustion engines [4, 5]. In fact, hydrogen has a wide flammability range (4% to 75% by volume in air), a high laminar flame speed of approximately 2 m/s, and requires very low ignition energy. In comparison, conventional fuels such as diesel and gasoline have much narrower flammability limits, 0.6% to 7.5% for diesel and 1.4% to 7.6% for gasoline, and a laminar flame speed of around 40 cm/s for both. These properties make hydrogen particularly attractive for internal combustion engine applications, especially under ultra lean-burn conditions where conventional fuels struggle to ignite and propagate combustion efficiently [6,7].

In spark ignition engine [8], Hydrogen exhibits lower cyclic variations than other fuels, even in lean conditions, resulting in reduced emissions, improved efficiency, and smoother operation. Its high effective octane number is due to its fast-burning rate and low preignition reactivity. Mixed with gasoline [9], abnormal and incomplete combustions are reduced at low load, along with the covariance (CoV) of the indicated mean effective pressure (IMEP). Emissions of HC, CO, and CO_2 are also reduced with hydrogen addition, while NO_x tends to increase, mainly because of the high combustion temperature.

For compression ignition engines, one easy way to retrofit it is to ignite hydrogen by a diesel pilot injection, reducing CO_2 emissions and other carbon emissions such as CO, unburnt HC and soot. Several studies on diesel-hydrogen dual-fuel (DF) engines cover various configurations, including single-cylinder engines [10-16] and larger engines, such as four-cylinder turbocharged ones [17-21]. However, a significant gap in literature exists regarding compression ignition (CI) engines for off-road application in this configuration, as proposed in this study.

In [13], authors observed that at low load, cyclic variation increases by increasing the amount of hydrogen. This is due to the decrease in diesel pilot content, which does not guarantee the main charge. For medium and high loads, increasing the amount of hydrogen does not have a significant impact on engine stability, maintaining the CoV from IMEP below 5%. Regarding maximum in-cylinder pressure, studies [10, 11, 13, 15, 20] reported an overall decrease of maximum pressure for low load due to the increase of the overall ignition delay while keeping the injection phasing constant, inducing a change in the combustion phasing as a function of the hydrogen content. Gaseous hydrogen also takes more place in the cylinder, reducing at the same time the volumetric efficiency of the engine. On the other hand, for medium and high load, the maximum pressure increases when more hydrogen is injected because the combustion is faster due to enhancement by hydrogen.

It is also noted that for these loads, the maximum pressure can be closer to top dead center (TDC), that enhances the increase of pressure because the energy is released near the smallest volume. Finally, concerning the rate of heat release (ROHR), studies reported earlier and lower peak of heat release at low load, and earlier and higher heat release at high load while increasing the amount of hydrogen. These findings are explained also by the faster combustion of hydrogen, which leads to earlier heat release. In [21], a clear difference in ROHR and combustion characteristics when moving from hydrogen equivalence ratios (EQR) below 0.1 to those above it. When EQR is less than 0.1, combustion remains dominated by diesel spray processes with minimal impact from hydrogen. However, once EQR exceeds 0.1, to a significant increase in ROHR due to the onset of premixed hydrogen-air flame propagation, resulting in faster and earlier combustion.

The emissions are also strongly affected by hydrogen combustion. As expected, a consistent reduction in CO_2 emissions across all loads [10-15, 18] is obtained, attributed to hydrogen's carbon-free nature and the decreased need for diesel, leading to a higher hydrogen-to-carbon (H/C) ratio. Additionally, hydrogen's high diffusion coefficient results in better premixed and uniform mixtures, reducing heterogeneity in diesel fuel spray and enhancing combustion efficiency. For most of the cases, the particulate matter (PM) observed an overall decrease for all loads since increasing the hydrogen quantity leads to a decrease of diesel fuel consumption that reduced significantly the amount of carbon in the mixture [10-16, 18]. However, for high load, some studies noticed an increase in the soot as in [13]. Finally, in [11] the PM number increases as the hydrogen/air mixture is richer without reducing the diesel content. Nitrogen oxides (NO_x) emissions [10, 17, 18, 19] exhibit varied behavior depending on the load: a decrease in NO_x emissions at low loads due to lower combustion temperatures; but at high loads, NO_x emissions tend to increase, driven by higher combustion temperatures and longer residence times. At mid loads, the trend is less consistent, with NO_x emissions either increasing or decreasing depending on the amount of hydrogen and the experimental configuration.

The aim of this study is to investigate experimentally the potential of hydrogen-diesel combustion in a 3-cylinder ,1 liter, CR 17.5 engine, as a function of the load by increasing the hydrogen content, while keeping the diesel part as the ignition source. This is achieved through a simple retrofit solution, where only the hydrogen injection parameters are adjustable while diesel injection is controlled by the engine's ECU. Combustion characteristics and emissions are studied and the feasibility of retrofitting the engine using this straightforward method will be evaluated.

Setup and experimental procedure

Experimental setup

As previously mentioned in the introduction, the engine used in present experimental work is a 3-cylinder, 1-liter, CI engine. It was converted to run in dual fuel configuration by adding PFI injectors near the intake valves. The main characteristics of the engine are listed in Table 1.

Table 1. General characteristics of the engines

Engine characteristics	
Engine type	Compression ignition
Number of cylinders	3, in-line
Bore [mm]	75.0
Stroke [mm]	77.6
Total displacement [cm^3]	1028
Diesel injection system	Direct, common rail
Aspiration	Naturally aspirated
Compression ratio	17.5:1
Max. power [kW]	15 @ 3600 rpm
Max. torque [Nm]	60 @ 2000 rpm
Intake valves opening [cad BTDC]	13°
Intake valves closing [cad ABDC]	39°
Exhaust valves opening [cad BBDC]	38°
Exhaust valves closing [cad ATDC]	14°

The schematic of the experimental setup is represented in Figure 1. In appendix Table A1, the full list of the sensors is provided with their range and precision.

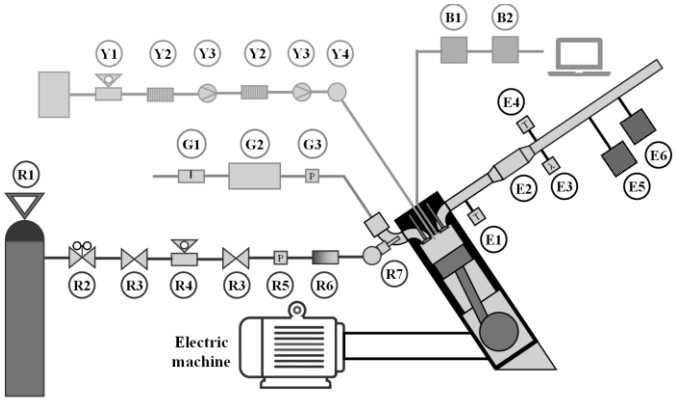

Figure 1. Schematic of the experimental setup

The engine was linked to an electrical machine and is mounted at a 34° angle relative to the vertical, reflecting the geometry of the oil pan and how the engine is positioned in the vehicle, which is a 4-wheel off-road vehicle, belonging to the L7 category [22]. Due to this inclination, special attention is required when operating in dual fuel configuration. Since hydrogen combustion produces mainly water, there is a risk that water vapor could accumulate in the exhaust manifold. To prevent potential issues when shutting down the engine, diesel alone is maintained for several minutes before stopping. This allows any trapped water vapor to be cleared from the exhaust manifold. Additionally, the original engine's ECU is locked, meaning that it is impossible to modify any internal settings such as the timing, duration or splitting of the diesel injection. In this study, no Exhaust Gas Recirculation (EGR) was used.

For the diesel line, shown in yellow in Figure 1, a Coriolis mass flow meter (Y1) from Emerson, a CMF010M with a resolution of 0.036 kg/h and maximum range of 81.65 kg/h, is used to measure the diesel mass flow rate. The diesel then passes through filters (Y2) and both low- and high-pressure pumps (Y3), which are connected to the common rail (Y4). To accurately monitor diesel injection, a Hall effect sensor was mounted on the injector wire of the cylinder closest to the flywheel.

For the air line, in green in Figure 2, a hot wire sensor (G1) from EYC-TECH, the FTM06D-1 with a resolution of 0.01 m^3/h and maximum range of 848 m^3/h, measures the velocity, temperature, and pressure, to determine the mass flow rate of air entering the engine. A plenum (G2) is set to reduce pressure fluctuations during engine operation. A relative pressure sensor (G3) from Valcom, a 27A Series with an accuracy of 0.001 bar, is installed in the intake manifold to monitor pressure variations.

The hydrogen line, in red in Figure 1, begins with a 200-bar gaseous hydrogen bottle (R1) connected to a pressure regulator (R2) that reduces the pressure to 5 bar. A Coriolis mass flow meter (R4) from Emerson, a CMFS015M with a resolution of 0.093 kg/h and maximum range of 310.20 kg/h, measures the hydrogen flow rate, with two safety valves (R3) in place to ensure safe operation. Additionally, a flame arrestor (R6) prevents backfire, and two pressure sensors are installed: one on the line (R5) and another on the hydrogen rail (R7). As illustrated in Figure 2, the hydrogen rail has three Bosch port-fuel injectors typically used for PFI gas system each aligned with an intake valve, along with a temperature sensor. The hydrogen flow rate per injector is 1700 cc/min at 4 bars. Additionally, the hydrogen injectors are controlled using a delay unit that generates the signals to command hydrogen injection. A hydrogen sensor (Sintesy S210.smartSensor), which measures the percentage of the Lower Explosive Limit (LEL), was also installed near the engine to detect any potential leakage and ensure safety during operation.

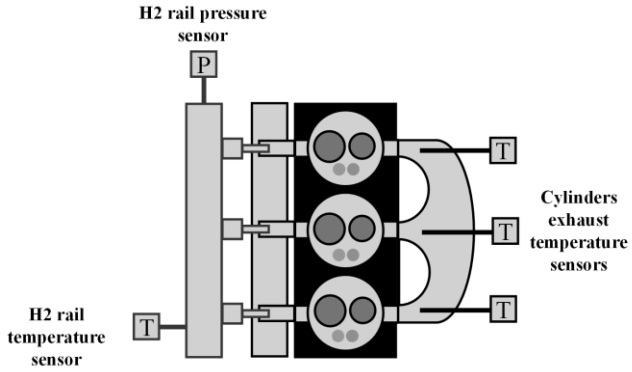

Figure 2. Detailed view of the sensors near the engine

Each cylinder is equipped with a pressure transducer, connected to a signal amplifier (B1) and to a signal acquisition system (B2), both provided by AVL.

As shown in Figures 1 and 2, each exhaust line is equipped with a temperature sensor (E1) mounted on the exhaust manifold. The exhaust system includes a Diesel Oxidation Catalyst (DOC, E2), a lambda sensor (E3) to measure the oxygen content in the exhaust gases, with an

adjacent temperature sensor (E4). Additionally, two exhaust analysis systems are used: an AVL DiTEST GAS 1000 (E5), for measuring CO (accuracy: 0.03% vol), CO_2 (accuracy: 0.5% vol), NO_x (accuracy: 50% ppm vol), O_2 (accuracy: 5% vol), HC (accuracy: 10% ppm vol) and Lambda (calculated from CO, CO2, HC and O2); and an AVL Smoke Meter 415S (E6) to assess smoke levels (accuracy: 3% of the measured value FSN). These two exhaust gas analyzers are monitored using software specific to the respective system. Furthermore, several temperature sensors are installed to monitor the engine's coolant temperature as well as the temperature of the cooling water used to regulate the temperature of the engine's coolant.

To acquire data from all the sensors, several software tools are used. For slow data acquisition, such as monitoring temperature, pressure and some mass flow rate, LabVIEW is utilized. For fast data acquisition, including in-cylinder pressure, mass flow rates of hydrogen and diesel, and the signals from the hydrogen injectors are monitored by AVL Indicom which also provides combustion analysis (Coefficient of Variation (COV), Rate of Heat Release (ROHR), the crank-angle where % of burnt mass fraction is (CA50) and combustion duration).

Experimental procedure

For the experiments, the engine was first warmed up until the coolant temperature reached 78°C. The intake air was maintained at 25°C with 35% humidity. The Exhaust Gas Recirculation (EGR) valve was mechanically deactivated, and a Diesel Oxidation Catalyst (DOC) was installed to prevent any hydrogen combustion in the exhaust. Measurements were taken at 6 different engine speeds, ranging from 1600 rpm to 3600 rpm increments in 400 rpm, and at 3 different loads: 30%, 50%, and 70% of the maximum torque output. In dual-fuel mode, 10% of the total torque output for each engine speed (5 Nm) is provided by diesel as the ignition source for hydrogen. Before running the engine in dual-fuel mode, it was operated at 10% load using only diesel to establish baseline data for comparison. For all the tests, the diesel injection strategy is the one from the engine's ECU, and as we cannot change the settings, the diesel injection will remain separated in two, with a pre and a main injection, with the pattern presented in Table 2. From this table, it can be observed that pilot injections represent around 40% of the total diesel injection at each load, considering that the injection pressure for all conditions at 10% of load is fixed at 400 bar.

Table 2. Diesel injection timing

Engine speed [rpm]	SOI pilot [CAD]	DOI pilot [µs]	SOI main [CAD]	SOI main [µs]
1600	-10,4	354	2,6	438
2000	-12,8	350	2,2	417
2400	-15,6	361	0,4	458
2800	-22,2	333	-4	452
3200	-32,8	333	-10,4	510
3600	-39	324	-12	537

Table 3 presents key parameters of the tested operating points for both diesel-only and dual fuel operation. The premixed air-fuel ratio (λ) is calculated as in Eq. 1, Hydrogen Energy Share (HES) as in Eq. 2 and Indicated Mean Effective Pressure was computed from the in-cylinder pressure signal as Eq. 3.

$$\lambda_{premixed} = \frac{\dot{m}_{air}}{AFR_{H_2}^{st} * \dot{m}_{H_2}} \quad (1)$$

Where $\dot{m}_{H_2}, \dot{m}_{Diesel}, \dot{m}_{air}$ = mass flow rates of hydrogen, diesel and air, respectively in kg/h.

$$HES = \frac{\dot{m}_{H_2} * LHV_{H_2}}{\dot{m}_{H_2} * LHV_{H_2} + \dot{m}_{Diesel} * LHV_{Diesel}} * 100 \quad (2)$$

Where LHV_{H_2} and LHV_{Diesel} = LHV of hydrogen and diesel in kJ/kg.

$$IMEP(bar) = \frac{\int p * dV}{V_d} \quad (3)$$

Where p = in-cylinder pressure (bar) and V_d = Displacement volume for one cylinder (m^3).

Table 3. Campaign test points

Fuel	Engine Speed [RPM]	Load [%]	Premixed lambda	HES [%]
Diesel	1600	10	-	-
	2000			
	2400			
	2800			
	3200			
	3600			
Dual-Fuel Diesel - H2	1600	30 - 50 - 70	6,71 - 4,2 - 3,57	52 - 65 - 65
	2000		6,15 - 4,46 - 3,66	53 - 59 - 64
	2400		7,01 - 4,94 - 3,91	47 - 57 - 60
	2800		7,71 - 5,62 - 3,91	46 - 54 - 59
	3200		6,35 - 4,79 - 4,13	40 - 47 - 49
	3600		6,13 - 5,69 - 4,67	39 - 40 - 42

To prevent unburned hydrogen from being expelled through the exhaust, avoid backfire, and ensure no hydrogen remains in the intake manifold, the hydrogen injection is initiated at -346° CAD, just after the exhaust valve closing (EVC) and the intake valve opening (IVO) as the valve lift diagram indicated in Figure 3. The Exhaust Valve Opening (EVO), Exhaust Valve Closing (EVC), Intake Valve Opening (IVO), and Intake Valve Closing (IVC) are represented in the lift diagram. The black curve shows the piston position throughout the four strokes, the red curve represents the lift of the exhaust valve, and the blue curve indicates the lift of the intake valve. Injections can continue until 141° CAD before the top dead center, providing a maximum possible injection duration of 205°. However, for the purposes of this experiment, such a long injection duration was not necessary.

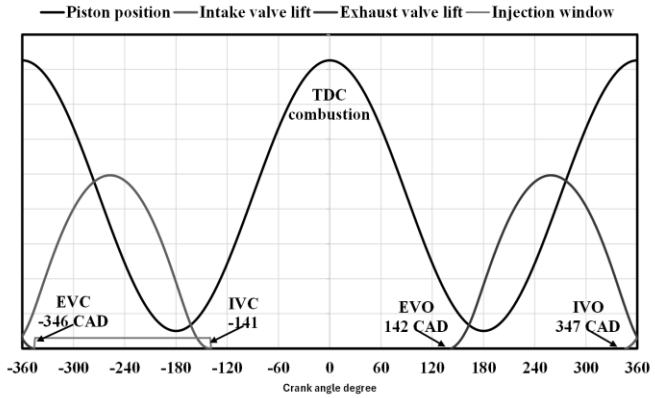

Figure 3. Valves lift diagram

Prior to collecting data at each test point, the exhaust temperature of each cylinder was stabilized to ensure proper hydrogen injection and a steady operating condition.

The coefficient of variation (COV) was computed from the IMEP averaged over 200 cycles. From the in-cylinder pressure signal, the gross rate of heat release (ROHR) is also computed, to estimate the efficiency and the CA50, the crank angle where 50% of the fuel has burned. For this engine, an optimal combustion efficiency typically occurs when CA50 is phased around 14° after top dead center (ATDC). Last, the exhaust gas temperature is also monitored, to provide an indication of the level of heat generated during combustion and helps assessing pollutant formation trends, such as the potential rise in NO_x emissions under high-temperature conditions. During the study, only emissions of

particulate matter (PM), CO_2 and NO_x are provided, as the sampling is done after Diesel Oxidation Catalyst to reduce CO and unburnt HC emissions.

Results and discussion

In all the following figures, the following labels are used, defined as:

- D_10 refers to the operation of the engine with only diesel at 10% of the full load. (black)
- DF_30 refers to the engine operating under diesel/hydrogen dual-fuel mode at 30% of the full load. (red)
- DF_50 refers to the engine operating under diesel/hydrogen dual-fuel mode at 50% of the full load. (blue)
- DF_70 refers to the engine operating under diesel/hydrogen dual-fuel mode at 70% of the full load. (green)

Combustion characteristics

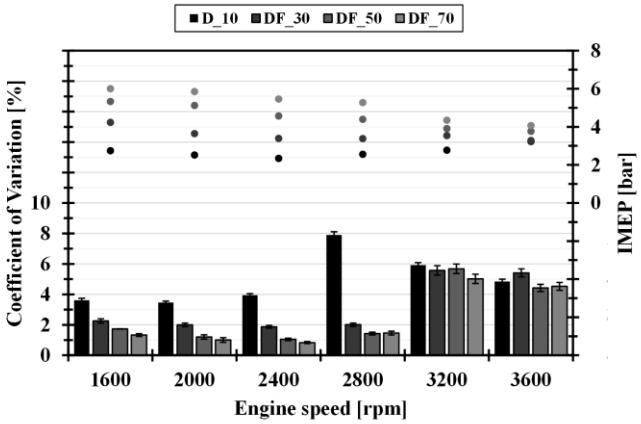

Figure 4. Coefficient of variation from IMEP (bars and left axis) and IMEP (dots and right axis)

The CoV_{IMEP} is plotted in Figure 4, with error bars indicating $\mp 2\sigma$ of the CoV_{IMEP} computed over 200 cycles. From 1600 to 2800 rpm, the highest CoV was always obtained for diesel only as it is a case of 10% load, that represents a very low torque demand and increasing the combustion instability. The hydrogen addition induces an increase in load, which results in an improvement of combustion stability. On the other hand, for the engine speed of 3200 and 3600 rpm, the CoV is less affected by the hydrogen addition even if the IMEP increases. In fact, this is due to suboptimal diesel injection phasing, which affects CA50 as plotted in Figure 5. For this engine, an optimal combustion phasing is considered when CA50 is close to 14 CAD a TDC.

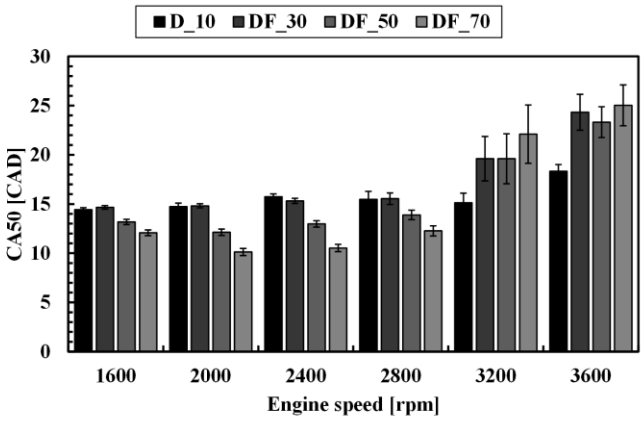

Figure 5. CA50 in crank angle degree ATDC

Indeed, for engine speed between 1600 rpm and 2800 rpm, CA50 occurs earlier as the load increases, due to the enhancement of the combustion development speed by hydrogen. Therefore, it suggests that retrofitting the engine in dual fuel operation, without modifying the diesel injection timing, could be a viable solution while maintaining combustion stability. However, at 3200 rpm and 3600 rpm, increasing the load results in a delayed CA50. In fact, despite the advanced diesel injection, the combustion of the mixture occurs during the expansion stroke, in a larger cylinder volume. This indicates the slowdown of the overall burn rate, despite the presence of hydrogen. This delayed CA50 may result in suboptimization of the combustion, increasing exhaust temperature, and therefore emissions. For these engine speeds, retrofitting the engine without adjusting the diesel injection timing is not feasible. However, different operating conditions such as increasing the diesel load from 10% to 20% could help to ignite hydrogen and advance the combustion phasing.

The in-cylinder pressure, rate of heat release and the current that controls the diesel injector are represented in Figure 6, for the engine speed of 2400 rpm. For this engine speed, the diesel injection was fixed as follows:

- SOI_{pilot} at -15.6 CAD ATDC with a duration of 361 μs
- SOI_{main} at 0.4 CAD ATDC with a duration of 458 μs

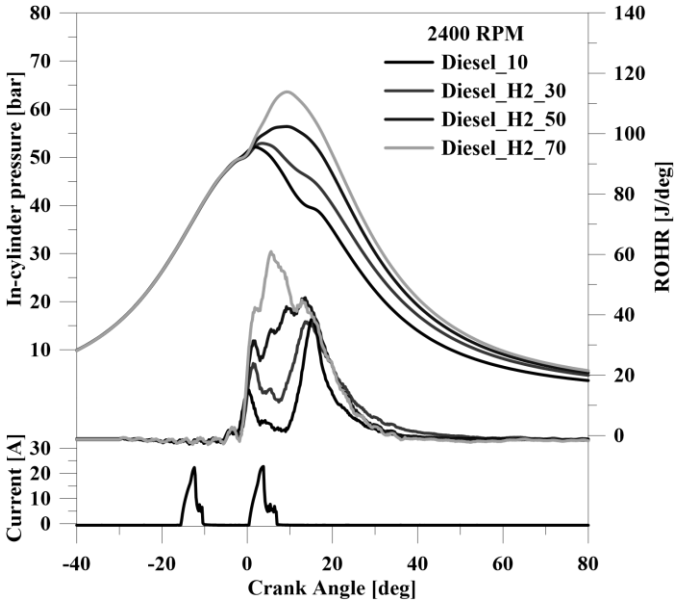

Figure 6. In-cylinder pressure and ROHR at 2400 rpm and several loads

For all operating conditions, the first start of combustion is maintained certainly due to the diesel ignition only. However, for 30% load (red curves), the hydrogen content needs the second injection of diesel to completely burnt. At this condition, the energy given by the hydrogen is HES = 47% with a global air excess, l = 7.01. The ROHR peaks are well aligned with those obtained with diesel-only. At 50% load (in blue), the combustion of hydrogen follows the first diesel combustion peak until the second maximum of ROHR enhanced by the second diesel injection. At this condition the hydrogen/air mixture is less lean, as the amount of diesel injected is constant (l = 4.94), and HES is higher (57%). At 70% load (in green), even if the first peak due to the combustion of the first charge of diesel is distinguishable, the ROHR continues to grow, enhanced by the increase of HES (60%.) even if l = 3.91. The main content of hydrogen is burnt before the second injection of diesel as ROHR decreases until the second diesel charge combustion. The phase with the second injection indicates that certainly no more hydrogen is available and only the main diesel is burning here. Nonetheless, it must be noted that when hydrogen is added, ROHR indicated that some hydrogen continues to burn after the second diesel peak, perhaps due to some trapped hydrogen by squish zone, due to the bowl shape of the piston.

Therefore, from this example, retrofitting this engine with hydrogen appears to work effectively: at low load, the splitting of the diesel injection facilitates the combustion of hydrogen share without affecting significantly the phasing of the ROHR. This ensures that the combustion phasing remains optimal. However, for medium and high loads, after the first diesel combustion ignites the hydrogen/air mixture, hydrogen can burn on its own, which can lead to change in the combustion phasing. The overall optimization must be done for all loads/engine speed by adapting also the diesel injection timing itself and injection strategies (one or multiple injections).

The data, represented in Figure 7, are at a higher engine speed of 2800 rpm. In this configuration, the diesel injection is fixed as follows:

- SOI_{pilot} at -22.2 CAD ATDC with a duration of 333 μs
- SOI_{main} at -4 CAD ATDC with a duration of 452 μs

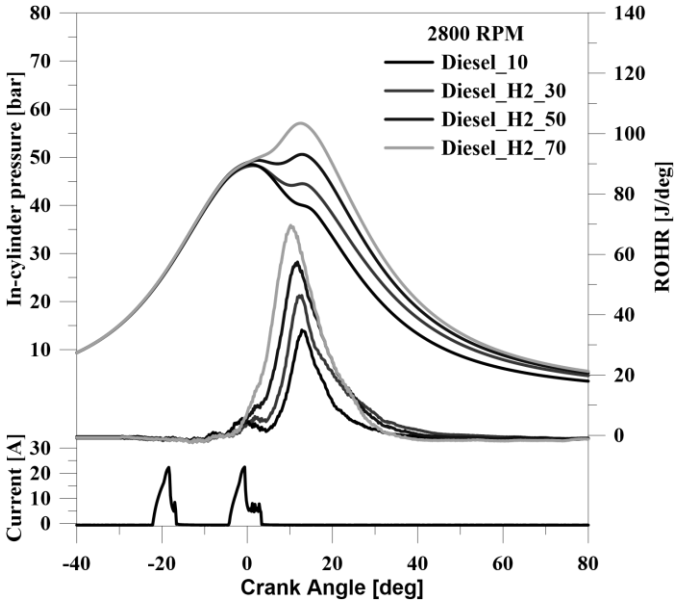

Figure 7. In-cylinder pressure and ROHR at 2800 rpm and several loads

At this engine speed, like the previous one, the first start of combustion is maintained thanks to diesel ignition, for all the loads. As the engine speed is higher, the time between the two diesel injections is shorter, meaning less delay between the end of pilot combustion and the start of main combustion. As the load increases, the peak of heat release is shifting closer to the TDC, that indicates that hydrogen is burning on its own after the first ignition due to its high flame velocity, the mixture is burning quicker, that advances the peak of heat release. For 30% load (in red), hydrogen energy represents 46% with a global air excess of l = 7.71. Compared to 2400 rpm, slightly more energy is provided by diesel, and the overall mixture has the same equivalence ratio, so more energy is given at the start of combustion of hydrogen, that could explain why hydrogen is able to sustain combustion after the first ignition. The rate of heat release peak of DFH2 appears at 12 CAD ATDC compared to 13 CAD ATDC for diesel only operation at 10% load. For 50% load (in blue), HES was 54% with a global air excess of l = 5.62. For this load, the rate of heat release peak was at 11 CAD ATDC. Finally, for 70% of the load, with a HES of 59% and l = 4.43, the peak was reached at 10 CAD ATDC.

From this engine speed analysis, it can be concluded that retrofitting the engine with hydrogen works properly. However, some adjustments concerning the diesel injection has to be made to optimize combustion phasing. Moreover, from Figure 7, it seems that only one injection of diesel can be sufficient to run the engine, at least for the tested conditions.

For the engine speed of 3200 represented in Figure 8, the diesel injections are set as below:

- SOI_{pilot} at -32.8 CAD ATDC with a duration of 333 µs
- SOI_{main} at -10.4 CAD ATDC with a duration of 510 µs
-

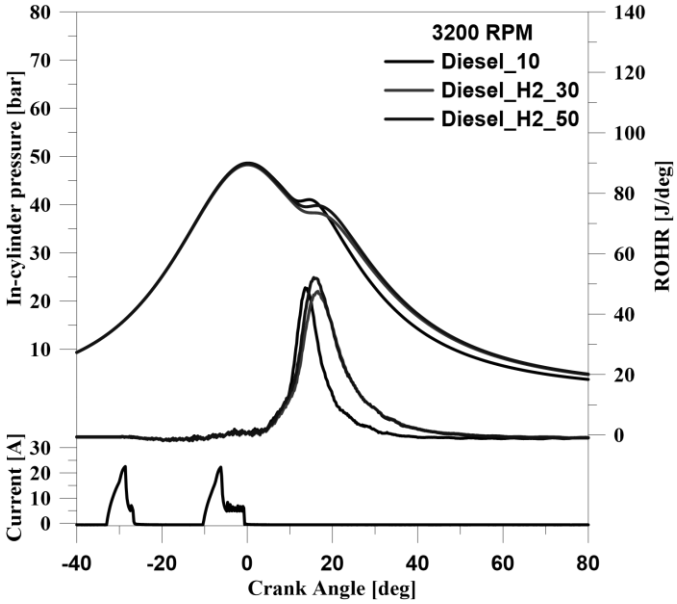

Figure 8. In-cylinder pressure and ROHR at 3200 rpm and several loads

At 3200 rpm, combustion occurs significantly after TDC, with in-cylinder pressure rising late during the expansion stroke for all conditions. The rate of heat release (ROHR) shows that even with hydrogen addition, the peak heat release remains nearly identical to the 10% diesel-only baseline and is slightly delayed. For the 30% load case (λ = 9.4, HES = 40%), the ROHR peak occurs at 16.4 CAD aTDC, compared to 13.6 CAD aTDC for the diesel-only case. A similar trend is observed for the 50% load case (λ = 9.1, HES = 47%), with a peak at 15.6 CAD aTDC. In both cases, only the broader ROHR profile suggests a possible contribution from hydrogen combustion. The 70% load case was not recorded to avoid the risk of unburned hydrogen reaching the exhaust and causing unwanted combustion events.

This poor combustion phasing results from the engine control unit (ECU) calibration, originally developed for operation with EGR. Since EGR was disconnected in this study, the diesel injection timing is no longer optimized for the current configuration. As a result, the hydrogen retrofit does not function effectively at this engine speed or above (up to 3600 rpm). To enable stable and efficient operation, further work is required to recalibrate diesel injection phasing and optimize the overall combustion process.

From the ROHR data in the previous figures, it can be observed that the addition of hydrogen influences combustion duration depending on the load, engine speed, and test conditions. This effect is illustrated in Figure 9 below, which presents the total combustion duration in crank angle degrees (CA90 – CA10) along with the distribution between the first half of combustion (CA50 – CA10) and the second half (CA90 – CA50).

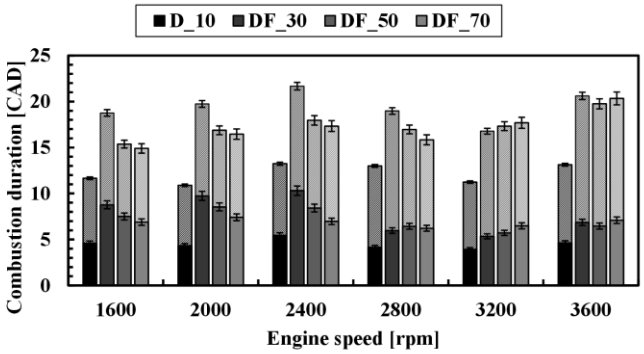

Figure 9. Combustion duration CA 90- CA10 in CAD. Full color bars represent CA50 - CA10 and stripped bars represent CA90 – CA50.

From Figure 9, it can be observed that for every tested point, the first phase of combustion (CA50 – CA10) is always faster than the second phase (CA90 – CA50). At a fixed engine speed, the combustion duration in diesel-only operation is consistently shorter, as only a small amount of fuel is injected. Between 1600 rpm and 2800 rpm, at 30% load, the combustion duration increases due to the higher fuel quantity. However, as the load increases to 50% and 70%, the combustion duration decreases, as seen in Figure 7, where the green curves (70% load) reach zero ROHR before the other dual-fuel cases. This trend depends on in-cylinder conditions, such as the excess air ratio and the ability of hydrogen to sustain combustion independently. At higher engine speeds (3200 rpm and 3600 rpm), no clear trend is observed when increasing the

hydrogen fraction, suggesting that additional factors, such as turbulence, mixture formation, and ignition characteristics, influence the combustion process at these speeds.

Emission characteristics

Emissions were monitored following stabilization of exhaust temperatures in the three cylinders and post-DOC location. However, the temperatures of the DOC continued to rise at engine speeds of 3200 rpm and 3600 rpm, exceeding cylinder exhaust temperatures by 60°C. This suggests a potential exothermic reaction occurring within the DOC, where unburned hydrogen, resulting from poor combustion phasing at these engine speeds, may burn inside the DOC and distort gas analyzer readings. However, this phenomenon could not be confirmed, as no hydrogen measurements were taken in the exhaust line. As a result, emissions data at these engine speeds are omitted from the analysis. Furthermore, due to the impact of the DOC, hydrocarbon (HC) and carbon monoxide (CO) emissions will not be included in the report, as they do not accurately represent the engine's raw exhaust gases. This limitation hinders an accurate evaluation of the true advantages of retrofitting an engine for diesel-hydrogen dual-fuel operation. Finally, the emission in dual fuel configuration will be compared with the pollutants emitted by the engine fueled with only diesel at fixed load. Subsequent results will present a comparative analysis between diesel and diesel-hydrogen dual-fuel operation under varying loads and engine speeds.

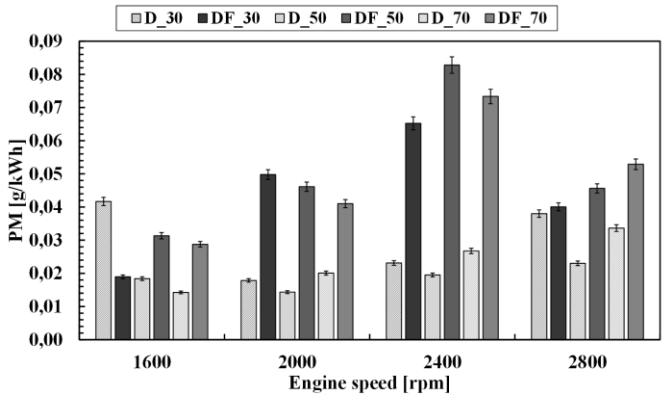

Figure 10. PM emissions in g/kWh for several engine speeds and loads

The emissions of particulate matter (PM) are displayed in Figure 10. A general trend of increasing PM production is observed across all engine loads and speeds, except for a significant 54% reduction at 1600 rpm and 30% load. The most notable increase in PM emissions occurs at 2400 rpm and 50% load during dual-fuel operation, showing a 77% rise compared to diesel-only operation.

The rise in PM formation can be attributed to various factors, despite hydrogen's absence of carbon. The displacement of air by hydrogen may lead to a reduction in diesel spray penetration and atomization, creating localized fuel-rich areas where PM is generated. Moreover, a high level of hydrogen substitution reduces the available air for diesel combustion, resulting in concentrated rich regions that facilitate soot formation. Additionally, the high ignition delay and rapid flame speed of hydrogen can modify the combustion process of the diesel spray, potentially cause local extinguishing and increase the formation of soot precursors. Another potential source of PM could be oil. Further analysis is necessary to investigate this phenomenon. One possible approach could involve the utilization of an Engine Exhaust Particle Sizer (EEPS) to measure particle size and quantity, combined with soot trapping followed by transmission electron microscopy (TEM) analysis to identify the origin of the PM.

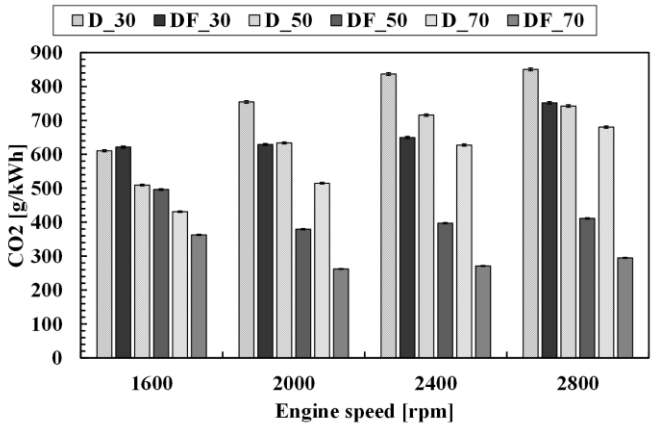

Figure 11. CO_2 emissions in g/kWh for several engine speeds and loads

Figure 11 displays the level of CO_2 emissions in g/kWh. When operating in dual-fuel mode, there is a general decrease in CO_2 emissions across all loads, except for a slight 2% increase noted at 1600 rpm and 30% load. In this case, it is difficult to determine the cause of the slight increase, as no measurements were taken in the raw exhaust gases upstream of the DOC. Since reactions can occur within the DOC, the exact nature of these reactions, especially when hydrogen is added, remains unknown. The most substantial reduction, at 57%, is observed at 2400 rpm and 2800 rpm with a 70% load. In comparison to diesel-only operation at a consistent load, CO_2 emissions are reduced in dual-fuel mode due to the lower injection of diesel. Since hydrogen does not contain carbon, its combustion does not contribute to the formation of CO_2. Within dual-fuel operation, an increase in load results in a decrease in CO_2 emissions. This is attributed to the constant amount of diesel injected across all loads, while the rise in load corresponds to an increase in engine power output, thereby reducing CO_2 emissions per unit of work.

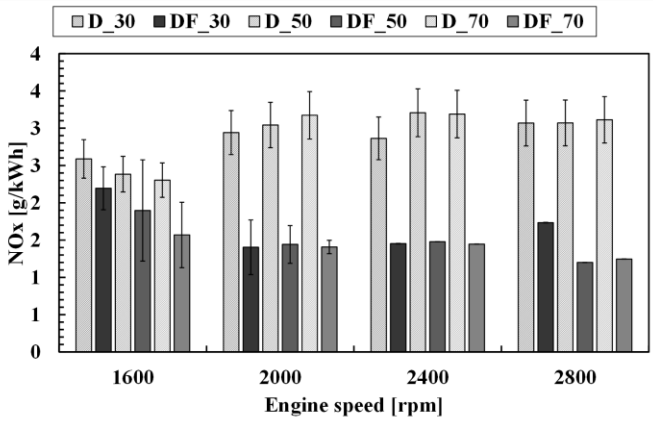

Figure 12. NO_x emissions in g/kWh for several engine speeds and loads

Figure 11 shows the NO_x emissions in grams per kilowatt-hour (g/kWh). In dual-fuel operation, NO_x emissions are consistently lower across various loads and engine speeds, with reductions of up to 61% observed at 2800 rpm and 50% load.

The decrease in NO_x production during dual-fuel mode can be attributed to several factors. One factor is that hydrogen displaces intake air, thereby reducing the oxygen available during combustion and limiting NO_x formation. For the tested conditions, a reduction up to 8% of the flow rate of air was achieved when adding hydrogen for DF operations. Additionally, hydrogen mixes more effectively with air compared to diesel, leading to a more uniform combustion process. This results in a more evenly distributed heat release and lower local peak temperatures. Since high temperatures are the primary driver behind NO_x formation, this decrease in peak combustion temperature helps mitigate NO_x emissions.

Previous research, such as [10], has demonstrated promising results with EGR in similar contexts to reduce NO_x emissions. Another possibility is switching to renewable diesel fuels, such as [8], like HVO (Hydrotreated Vegetable Oil), farnesane or methanol, which are cleaner alternatives and could help lower exhaust emissions, especially PM emissions.

Conclusions

This study focused on the combustion characteristics and emissions of a 1liter, 3-cylinder Naturally Aspired engine for off-raod applications, retrofitted to operate in dual fuel mode. The diesel charge parameter was fixed and only the optimization had been done through the control of the hydrogen injection parameters (phasing and duration).
This study presents promising results: the straightforward retrofit of a conventional engine proves effective, maintaining engine behavior while achieving a 57% reduction in CO_2 emissions compared to diesel-only operation. However, further improvements are needed at higher engine speeds to enhance stability.
The main conclusions from this experimental study are as follows:

- As the diesel content was kept constant (10% of the full load), CoV_{IMEP} is reducing while the hydrogen content, i.e. the load, increases. However, for 3200 rpm and 3600 rpm, this reduction is less significant due to suboptimal combustion phasing.
- CA50 advanced towards TDC due to the enhancement of the combustion speed by hydrogen. Depending on the load, the phasing is still acceptable. This simple way to retrofit a diesel engine seems to be suitable in terms of combustion phasing when the engine speed remains below 3000 rpm. However, for higher engine speed (3200 rpm and 3600 rpm), the CA50 moved far from the TDC, leading to a suboptimal combustion phasing.
- The in-cylinder pressure and ROHR evolution, change as a function of the load and the equivalence ratio of the overall mixture. Hydrogen can sustain its combustion after the diesel pilot starts the combustion. The phasing of ROHR does not change sufficiently to deteriorate the phasing of combustion. This could suggest that the retrofit on this engine could be suitable, depending on the engine speed.
- Particulate Matter (PM) emissions increase across most engine loads and speeds, except for a 54% reduction at 1600 rpm and 30% load. The highest PM rise (77% at 2400 rpm and 50% load) suggests that hydrogen displaces air, reducing diesel spray mixing and forming localized fuel-rich zones where PM is generated. A possible contribution of lubricating oil to PM emissions should be further investigated.
- CO_2 emissions are reduced across all conditions in dual-fuel mode, except for a slight 2% increase at 1600 rpm and 30% load. The largest decrease (57%) is observed at 2400 rpm and 2800 rpm at 70% load due to the displacement of diesel by hydrogen. Since hydrogen is

carbon-free, its combustion does not contribute to CO_2 emissions. The higher the load, the lower the CO_2 emissions per unit of work, as the diesel amount remains constant while power output increases.

- NO_x emissions are consistently lower with dual-fuel operation, with a maximum reduction of 61% at 2800 rpm and 50% load. This is attributed to the reduced oxygen availability, limiting NO_x formation, and to hydrogen's better mixing with air, leading to a more uniform combustion process and lower peak temperatures.

To further explore and improve this first study, several possibilities could be considered. First, the optimization of the diesel injection strategy (timing, splitting …) can be one way to optimize the engine overall all operating. The use of EGR and HVO must be also evaluated to lower both NO_x and PM emissions but by guaranteeing stability and the efficiency of the engine.

References

1. European Commission. "Energy, Climate Change, Environment." Accessed August 18, 2024. https://commission.europa.eu/energy-climate-change-environment_en.
2. European Parliament Directorate General for Communication, *Greenhouse Gas Emissions by Country and Sector (infographic)* (European Parliament, published 7 March 2018, last updated 2 December 2024), consulted at https://www.europarl.europa.eu/topics/en/article/20180301STO98928/greenhouse-gas-emissions-by-country-and-sector-infographic.
3. Muhammad Ihsan Shahid, Anas Rao, Muhammad Farhan, Yongzheng Liu, et al. "Hydrogen production techniques and use of hydrogen in internal combustion engine: A comprehensive review." *Fuel* 378 (2024) https://doi.org/10.1016/j.fuel.2024.132769.
4. Levikhin, A. A., and A. A. Boryaev. "Physical Properties and Thermodynamic Characteristics of Hydrogen." *Heliyon* 10, no. 17 (2024): e36414. https://doi.org/10.1016/j.heliyon.2024.e36414.
5. "Hydrogen." (Accessed August 23, 2024). Air Liquide Encyclopaedia, https://encyclopedia.airliquide.com/fr/hydrogene#properties
6. Gopinathan, R.L. and Ibrahim, M.M., "Ammonia as a Sustainable Fuel for Diesel Engines: Exploring Advanced Combustion Strategies for Green Transportation," *J. Energy Inst.* 121:102159, 2025, https://doi.org/10.1016/j.joei.2025.102159.
7. Sun, J., Zhao, N., and Zheng, H., "A Comprehensive Review of Ammonia Combustion: Fundamental Characteristics, Chemical Kinetics, and Applications in Energy Systems," *Fuel* 394:135135, 2025, https://doi.org/10.1016/j.fuel.2025.135135.
8. Karim, G. A. "Hydrogen as a Spark Ignition Engine Fuel." *International Journal of Hydrogen Energy* 28, no. 5 (2003): 569–577. https://doi.org/10.1016/S0360-3199(02)00150-7.
9. Duan, Xiongbo, Lining Feng, Liyan Feng, Xianghe Chu, Xingpeng Chu, and Zhiqiang Sun. "The Performance of a Spark Ignition Gasoline Engine with Hydrogen Addition under Low-Load Conditions." *Fuel* 379 (2025): 133091. https://doi.org/10.1016/j.fuel.2024.133091.
10. Saravanan, N., and G. Nagarajan. "Performance and Emission Studies on Port Injection of Hydrogen with Varied Flow Rates with Diesel as an Ignition Source." *Applied Energy* 87, no. 7 (2010): 2218–2229. https://doi.org/10.1016/j.apenergy.2010.01.014.
11. Karagöz, Yasin, Tarkan Sandalcı, Levent Yüksek, Ahmet Selim Dalkılıç, and Somchai Wongwises. "Effect of Hydrogen–Diesel Dual-Fuel Usage on Performance, Emissions, and Diesel Combustion in Diesel Engines." *Advances in Mechanical Engineering* 8, no. 8 (2016): 1–13. https://doi.org/10.1177/1687814016664458.
12. Bakar, R.A., Kadirgama, K., Ramasamy, D., Yusaf, T., Kamarulzaman, M.K., Sivaraos, A., Aslfattahi, N., Samylingam, L., and Alwayzy, S.H. "Experimental Analysis on the Performance, Combustion/Emission Characteristics of a DI Diesel Engine Using Hydrogen in Dual Fuel Mode." *International Journal of Hydrogen Energy* 52, no. 3 (2022): 843–860. https://doi.org/10.1016/j.ijhydene.2022.04.129.
13. Nag, Sarthak, Priybrat Sharma, Arpan Gupta, and Anish Dhar. "Experimental Study of Engine Performance and Emissions for Hydrogen Diesel Dual Fuel Engine with Exhaust Gas Recirculation." *International Journal of Hydrogen Energy* 44, no. 22 (2019): 12163–12175. https://doi.org/10.1016/j.ijhydene.2019.03.120.
14. Gültekin, N., and M. Ciniviz. "Examination of the Effect of Combustion Chamber Geometry and Mixing Ratio on Engine Performance and Emissions in a Hydrogen-Diesel Dual-Fuel Compression-Ignition Engine." *International Journal of Hydrogen Energy* 48, no. 66 (2023): 25984–25999. https://doi.org/10.1016/j.ijhydene.2023.03.328.
15. Pinto, G. M., de Souza, T. A. Z., Rocha, H. M. Z., Pereira, R. d. S., Nogueira, L. A. H., and Bakar, R. A. "A Review of the Use of Hydrogen in Compression Ignition Engines with Dual-Fuel Technology and Techniques for Reducing NOx Emissions." *International Journal of Hydrogen Energy* 48, no. 22 (2023): 19713–19732. https://doi.org/10.1016/j.ijhydene.2023.02.020.
16. A. Menaa, F. Amrouche, M.S. Lounici, K. Loubar. "Experimental investigation of hydrogen use in dual fuel and like dual fuel mode." *Fuel* 393, (2025), 135031. https://doi.org/10.1016/j.fuel.2025.135031.
17. Köse, Hüseyin, and Murat Ciniviz. "An Experimental Investigation of Effect on Diesel Engine Performance and Exhaust Emissions of Addition at Dual Fuel Mode of Hydrogen." Fuel Processing Technology 114 (2013): 26–34. https://doi.org/10.1016/j.fuproc.2013.03.023.
18. Castro, M. A., de Oliveira, L. S., de Lima, E. L., and de Oliveira, M. L. "An Experimental Investigation of the Performance and Emissions of a Hydrogen-Diesel Dual Fuel Compression Ignition Internal Combustion Engine." *Applied Thermal Engineering* 156 (2019): 660–669. https://doi.org/10.1016/j.applthermaleng.2019.04.078.
19. Akhtar, M. U. S., Asfand, F., Khan, M. I., Mishra, R., and Ball, A. D. "Performance and Emissions Characteristics of Hydrogen-Diesel Dual-Fuel Combustion for Heavy-Duty Engines." *International Journal of Hydrogen Energy* 50, no. 1 (2025): 1234–1245. https://doi.org/10.1016/j.ijhydene.2025.01.246.
20. Bakar, R.A., Kadirgama, K., Ramasamy, D., Yusaf, T., Kamarulzaman, M.K., Sivaraos, A., Aslfattahi, N., Samylingam, L., and Alwayzy, S.H. "Experimental Analysis on the Performance, Combustion/Emission Characteristics of a DI Diesel Engine Using Hydrogen in Dual Fuel Mode." *International Journal of Hydrogen Energy* 52, no. 3 (2022): 843–860. https://doi.org/10.1016/j.ijhydene.2022.04.129.
21. Reza Farzam et al., "Combustion Characterization and Heat Release Rate Modeling of a Heavy-Duty Hydrogen-Diesel Dual-Fuel Engine" (WCX SAE World Congress Experience, Detroit, Michigan, United States, 2025), 2025-01–8418, https://doi.org/10.4271/2025-01-8418.

22. European Alternative Fuels Observatory. "EU Classification of Vehicle Types." Accessed January 24, 2025. https://alternative-fuels-observatory.ec.europa.eu/general-information/vehicle-types.

Contact Information

Acknowledgments

The authors would like to thank Carlo Rossi and Bruno Sgammato, for the engine assessment and for support in the experimental activity. Also thank to Centro Nazionale per la Mobilità Sostenibile – CNMS, CN00000023 – Spoke 12 - CUP B43C22000440001 - DD MUR 1033 del 17/06/2022.

Definitions/Abbreviations

ABDC	After bottom dead center
ATDC	After top dead center
BBTD	Before bottom dead center
CI	Compression ignition
CO	Carbon moNOxide
CO_2	Carbon dioxide
CoV	Coefficient of variation
CR	Compression ratio
DI	Direct injection
DF	Dual fuel
EGR	Exhaust gas recirculation
EQR	hydrogen equivalence ratios
EVC	Exhaust valve closing
EVO	Exhaust valve opening
FSN	Filter smoke number
HC	Hydrocarbon
IMEP	Indicated mean effective pressure
IVC	Intake valve closing
IVO	Intake valve opening
LEL	Lower explosive limit
NA	Naturally aspirated
PFI	Port fuel injection
PM	Particle matter
ROHR	Rate of heat release
RPM	Revolution per minute
SOC	Start of combustion
SOI	Start of injection
TDC	Top dead center

Appendix

Table A1. List of the sensors used for the experiment

	Variable	Type of sensor	Brand	Model	Range	Resolution
Intake air	T° intake	Type K thermocuples	OGDEN	Series 121HT MGO	-200 - 1250°C	1°C
	P intake	Relative pressure sensor	Valcom	27A Series	-1 - 1 bar	0.001 bar
	Air mass flow rate	Hot wire	EYC-TECh	FTM06D-I	0.1 - 848 m3/h	0.01 m3/h
Hydrogen	H2 mass flow rate	Coriolis effect sensor	Emerson	CMFS015M	0 - 310,20 kg/h	0.093 kg/h
	P H2 rail	Absolute pressure sensor	Wika	Wika A-10	0 - 10 bar	0.001 bar
	P H2 line	Relative pressure sensor	GEMS	GEMS 795-4711	0 - 10 bar	0.001 bar
	T H2	Type K thermocuples	OGDEN	OGDEN series 121HT MGO	-200 - 1250°C	1°C
Diesel	Diesel mass flow	Coriolis effect sensor	Emerson	Emerson CMF010M	0 - 81.65 kg/h	0.036 kg/h
Engine	Torque	Dynamometer load cell	COMER	HS2 TETRAVEC 280.2	0 - 565 Nm	1 Nm
	Engine speed	Dynamometer load cell	COMER	HS2 TETRAVEC 280.2	7100 rpm	1 rpm
	Cylinder pressure	Quartz transducer	AVL	AVL GH14P-GH13P	0 - 250 bar	15pC/bar
	Signal amplifier	Amplifier pressure sensor	AVL	MICRO IFEM 4P4G	/	/
	Crank angle	Optical shaft encoder	AVL	AVL365C	0 - 20000 rpm	0,2 CAD
	Cycle	High-speed acquisition system	AVL	AVL Indimodul	/	0.2°
Coolant engine	T° out engine	Type K thermocuples	OGDEN	OGDEN series 121HT MGO	-200 - 1250°C	1°C
	T° in engine	Type K thermocuples	OGDEN	OGDEN series 121HT MGO	-200 - 1250°C	1°C
Cooling water	T° in exch	Type K thermocuples	OGDEN	OGDEN series 121HT MGO	-200 - 1250°C	1°C
	T° out exch	Type K thermocuples	OGDEN	OGDEN series 121HT MGO	-200 - 1250°C	1°C
	Water mass flow	Ultrasonic Flow Meter	Cynergy	UF25B	0 - 8 L/min	0.001 L/min
Exhaust	Lambda	Oxygen sensor	ETAS	ETAS Lambda Meter LA4	0 - 24,41 %	0,0001
	P exhaust	Relative pressure sensor	Valcom	27A Series	0 - 1 bar	0.001 bar
	T° cylinders	Type K thermocuples	OGDEN	OGDEN series 121HT MGO	-200 - 1250°C	1°C
	T° after DOC	Type K thermocuples	OGDEN	OGDEN series 121HT MGO	-200 - 1250°C	1°C
Exhaust gaz analyser	Smoke	Smoke meter	AVL	AVL smoke meter 415S	0 - 10 FSN	0.001 FSN
	CO	Emission tester	AVL	AVL DiTest Gas 1000	0 - 15 % vol.	0,01 % vol.
	CO2				0 - 20 % vol.	0,01 % vol.
	HC				0 - 30000 ppm vol.	1 ppm vol.
	NO				0 - 5000 ppm vol.	1 ppm vol.
	O2				0 - 25 % vol.	0,01 % vol.